Orientated Crystallization in Discontinuous Aramid Fiber/ Isotactic Polypropylene Composites under Shear Flow Conditions

Boris Larin,[1] Gad Marom,[1] Carlos A. Avila-Orta,[2,3] Rajesh H. Somani,[3] Benjamin S. Hsiao[3]

[1]*Casali Institute of Applied Chemistry, Institute of Chemistry, Hebrew University of Jerusalem, 91904 Jerusalem, Israel*
[2]*Departamento de Química de Polímeros, Centro de Investigación en Química Aplicada, Saltillo, Coahuila C.P. 25100, México*
[3]*Department of Chemistry, State University of New York at Stony Brook, Stony Brook, New York 11794-3400*

Received 7 February 2005; accepted 18 March 2005
DOI 10.1002/app.21926
Published online in Wiley InterScience (www.interscience.wiley.com).

ABSTRACT: Melt blends of short aramid fibers (AF) and isotactic polypropylene (iPP) are subjected to shear at 145°C and the structural evolution and final morphology are examined by *in situ* synchrotron X-ray scattering/diffraction and high-resolution scanning electron microscopy, respectively. The results indicate that the presence of short AFs significantly enhances the crystallization of iPP. It is argued that shear flow in this system exerts a twofold orientating action, namely, on the bulk iPP molecules and on the short AFs. The resultant crystalline morphology reflects the combined effects of crystallization on orientated iPP molecules to facilitate a shish kebab morphology and at the interface of the aligned fibers, to form transcrystallinity. © 2005 Wiley Periodicals, Inc. J Appl Polym Sci 98: 1113–1118, 2005

Key words: shear-flow-induced crystallization; aramid fiber; isotactic polypropylene blends; shish kebab morphology

INTRODUCTION

Flow conditions in polymer melts that contain acicular fillers, such as short fibers and whiskers, produce two main effects on the respective molten matrix and filler. The first is to promote chain disentanglement and create longer sequences of aligned chain segments,[1] and the second is to orientate the acicular filler parallel to the flow lines.[2] In turn, the aligned chain molecules and fibers both generate orientated crystalline morphology by two separate mechanisms. On the one hand, the aligned molecular arrays can act as nuclei for folded-chain crystallization with growth perpendicular to the flow direction, resulting in a shish kebab type morphology, in which the shish parts consist of aligned extended chains parallel to the flow direction, and the kebab parts are made of transversely grown lamellae.[3] On the other hand, the fibers, with a relatively high nucleus concentration at their surfaces, generate cylindrical transcrystallinity of preferential orientation with respect to the fiber direction.[4]

Correspondence to: G. Marom (gadm@vms.huji.ac.il).
Contract grant sponsor: Israel Science Foundation; contract grant number: 40/01.
Contract grant sponsor: National Science Foundation; contract grant number: DMR-0405432.

The phenomenon of flow-induced molecular orientation and crystallization has been studied quite extensively,[5–11] dealing with the effects of processing conditions (e.g., temperature, deformation rate, and strain) and polymer properties (e.g., molecular weight and distribution). The main factor that controls the flow-induced crystallization in polymers is the relaxation time of the deformed chains, which in turn depends on the flow rate and the chain molecular weight. Longer relaxation times are necessary for the formation of stable and oriented nuclei in the polymer melt, as in the case of deforming high molecular weight polymers under high deformation rates. Recently, several studies have been carried out to investigate the kinetics and morphological effects of different factors such as flow conditions, high molecular weight fractions, immiscible blends, and others on flow-induced crystallization in polymer melts. Relevant to the system investigated in this work, shear-induced crystallization in isotactic polypropylene (iPP) containing high molecular weight polyethylene (PE) oriented precursor domains, formed of chopped ultrahigh molecular weight PE (UHMWPE) fiber, has recently been investigated in our laboratories.[12] The results indicate that the presence of oriented UHMWPE domains significantly facilitated the crystallization of iPP and enhanced the initial shish kebab structure, leading to the final cylindritic morphology. It has been argued that shear flow orients the UHMWPE

domains, where the interfacial friction between PE and iPP effectively retards the relaxation of iPP chains, allowing the aligned iPP chains to create a shishlike structure.

At the same time the phenomenon of transcrystallization has been studied extensively in various fiber–matrix combinations, emphasizing the preferential orientation of the lamellae in the transcrystalline layer with respect to the fiber direction. Of particular relevance to the present work is a series of studies on transcrystallinity in aramid fiber (AF) reinforced iPP,[13–16] especially the one with emphasis on the structure of α transcrystallinity and the unique lamellar twisting morphology as a function of the distance from the fiber surface.[16]

The current study, which follows our recent works on iPP/PE blends,[17] attempts to assess the combined nucleating effect of the two simultaneous components, which are the aligned shish molecules and the orientated fibers, in a short fiber containing melt under shear flow conditions. Enhanced effects are expected on both the kinetics of crystallization and the level of orientation. These effects result in significantly shorter induction times for transcrystallization due to the shish molecules and fiber surfaces and form a highly orientated shish kebab morphology in association with transcrystallization, as shown in a microfibrillar poly(ethylene terephthalate)/polypropylene blend.[18]

EXPERIMENTAL

Materials

Melt-mixed polymer blends were composed of iPP (weight-average molecular weight = 127,000 g/mol, polydispersity = ~3.5, Basell) and 3 mm long chopped AFs (Kevlar 49, DuPont).

Sample preparations

Melt blending of iPP with 10 wt % chopped fibers (iPP/AF) was carried out in a twin-screw microcompounder (DACA Instruments). Blending was performed at 200°C in two consecutive 10-min cycles. Antioxidant (Irganox 3114, 5% w/w, Ciba) was added to prevent polymer degradation at high temperatures. The resulting blends were pressed in a mold to produce 0.5–1 mm thick films, from which ring specimens (internal diameter = 10 mm, width = 5 mm) were cut out by stamping for shear X-ray measurements.

Shearing conditions

A Linkam CSS-450 shearing stage was used to carry out the shear X-ray measurements. The stage consisted of two circular parallel plates (one stationary and the other rotated by a stepping motor) and two X-ray windows (diamond and Kapton) to allow *in situ* X-ray scattering/diffraction measurements. The temperature profile was precisely controlled by heating and cooling modules to an accuracy of ±0.2°C. The ring-shaped sample was sandwiched between two parallel plates of the stage, heated quickly to 200°C, held at this temperature for 5 min, followed by rapid cooling to 145°C, where shearing was imposed at a rate of 60 s^{-1} for 5 s. The melt was then allowed to isothermally crystallize for 1.0 h and cooled to room temperature at a rate of 30°C/min.

Wide-angle X-ray diffraction (WAXD) and small-angle X-ray scattering (SAXS) measurements

In situ SAXS and WAXD measurements were performed at Beamlines X3A2 and X27C, respectively, in the National Synchrotron Light Source, Brookhaven National Laboratory (Upton, NY). The details of the experimental conditions and setup have been described previously.[19] For WAXD measurements, the sample to detector distance was 125.5 mm using aluminum oxide (Al_2O_3) as a standard with a wavelength of 1.54 Å. For SAXS measurements, the sample to detector distance was 1688.2 mm using silver behenate as a standard with a wavelength of 1.36 Å. In both WAXD and SAXS measurements, a CCD camera from MAR-USA with a pixel size of 158 μm was used to collect the scattering data. Two-dimensional images were corrected for air scattering and beam fluctuations.

WAXD data analysis

The WAXD patterns were analyzed using Polar software (Stonybrook Technology and Applied Research Inc., Stonybrook, NY). The radially averaged and azimuthal intensity profiles of the principle diffraction peaks were extracted from every WAXD image. Origin software was used to plot the radial intensity profiles versus the Bragg angle (2θ), which was calculated using $2\theta = \tan^{-1}(R/D)$, where R is the diffraction ring radius and D is the sample to detector distance. The distance between the crystal planes (d) was calculated from the Bragg equation, $n\lambda = 2d\sin\theta$.

Scanning electron microscopy (SEM)

The sheared samples were etched following the Bassett procedure to highlight the crystalline structure.[20] The specimens were coated with a Au-Pd nanolayer by a SC7640 sputterer. EM experiments were carried out with a high-resolution scanning electron microscope (FEI Sirion) operated at 10 kV.

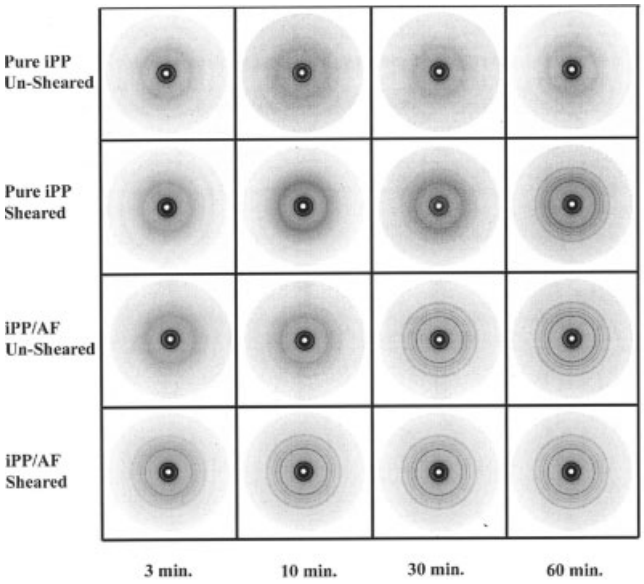

Figure 1 Selected *in situ* WAXD images of unsheared and sheared pure iPP and iPP/AF composites at varying crystallization times at 145°C.

Differential scanning calorimetry

Thermal analysis was carried out in a heating–cooling–heating cycle (Mettler DCS-30 calorimeter) at a heating/cooling rate of 10 K min^{-1} under nitrogen.

RESULTS

In the first part of this study, *in situ* WAXD and SAXS experiments were carried out to generate crystallographic, morphological, and kinetic data. Figure 1 presents a comparison of WAXD images taken at different times of isothermal crystallization at 145°C for sheared and unsheared samples of iPP and iPP/AF (10%, w/w). Concerning the pure iPP samples, there was no indication of crystallization even after 60 min; with shear, traces of a crystalline structure began to appear after 30 min and notable crystallinity was present after 60 min. The effect on the crystallinity of the short AFs was evident from the development of significant crystallinity after 10 min even without shear and 3 min after shear. Apparently, the sheared iPP/AF composite exhibited the shortest induction time, producing an oriented crystalline diffraction pattern at about 3 min after shear. All the diffraction patterns illustrated a pure α crystal form in iPP.[9] The crystal orientation was determined from the azimuthal profiles of the two-dimensional WAXD pattern (data not shown). Results indicated that the chains were aligned with respect to the flow direction, which was also consistent with the SAXS results later.

Figure 2 presents the corresponding SAXS patterns for the same materials as in Figure 1. The SAXS results were virtually identical to those of the WAXD, showing two extremes: no structural development even after 60 min in the unsheared iPP melt and rapid orientated morphological development after 2 min in the sheared iPP/AF melt. We found that the orientated lamellar structure was aligned perpendicularly to the flow, where the iPP chains were parallel to the flow. These observations confirmed that shear application was essential for inception of crystallization, as already reported.[3–8]

Differential scanning calorimetric analysis was performed to attempt to isolate the specific contributions of shear flow. Figure 3 presents the traces of two-cycle analyses of unsheared and sheared iPP/AF samples, showing the differences in the shape of the melting peaks. A comparison between the first melting scans of the unsheared and sheared samples revealed the effect of shear. Apparently, the onset of melting in the unsheared sample already occurred at 149°C with a shoulder around 155°C, whereas the onset of melting in the sheared sample was around 164°C with a sharp melting peak. It is also seen that shear resulted in an increase of the peak melting point from 163 to 169°C as well as an increase of the melting enthalpy from 70 to 74 J/g (corresponding to a small increase in the degree of crystallinity from 34 to 36%). The second scan, which followed cooling and recrystallization under quiescent conditions, reflected the crystalline structure after the shear effect was erased by the first melting scan. In this scan, the peak melting points and the degrees of crystallinity of the two samples became identical at 159°C and 34%.

SEM examinations of the etched surfaces provide important morphological information on the lamellar orientation in both bulk and interfacial iPP crystallinity. Although the main purpose of the SEM investigation is to analyze the morphology of the matrix at the vicinity of the fiber surface, the effect of shear on the bulk morphology of the matrix was clearly seen. Figure 4 illustrates a representative micrograph of the etched surface of a sheared iPP/AF sample, indicating the typical shish kebab morphology (shish and kebab structures can be identified parallel and perpendicular

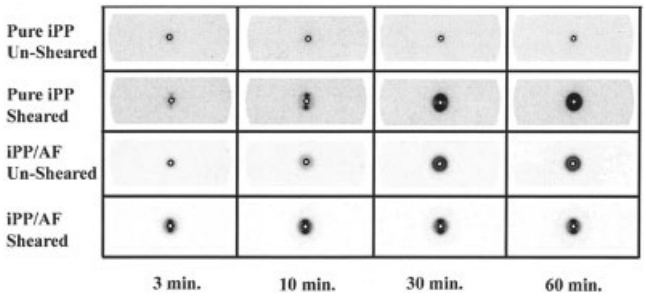

Figure 2 Selected *in situ* SAXS images of unsheared and sheared pure iPP and iPP/AF composites at varying crystallization times at 145°C.

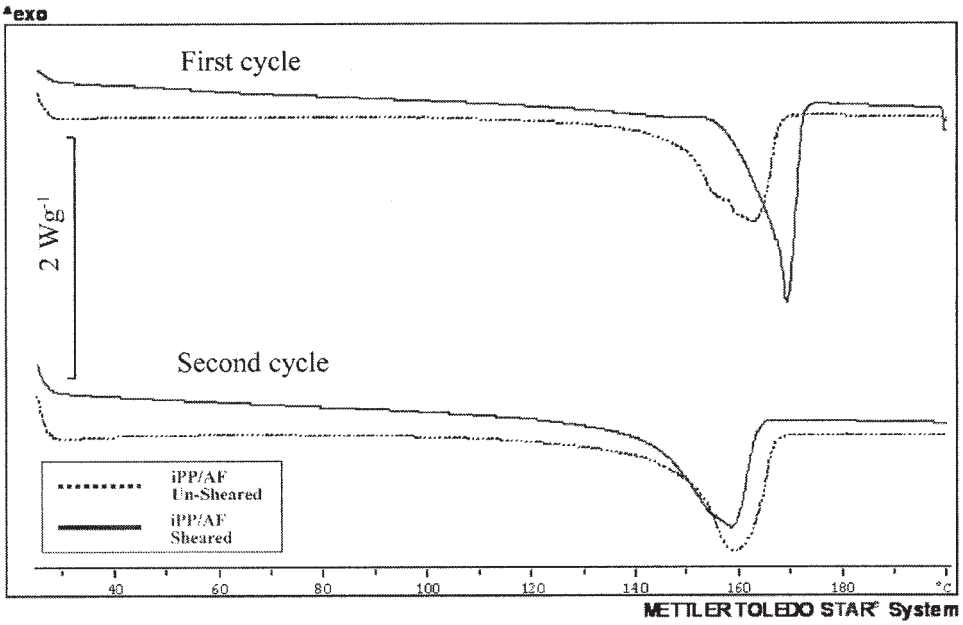

Figure 3 Differential scanning calorimetry traces of successive two-cycle analyses of unsheared and sheared iPP/AF composites, showing that the sheared sample loses its typical crystalline features after the first melting run.

to the flow direction, respectively). The examination of the interface was carried out on etched tapered cross sections, which exposed some fibers. Figure 5 shows a micrograph of such a fiber, which completely lost its circular shape because of the distorting effect of the melt-mixing process, and the iPP matrix at the vicinity of the surface. Two types of morphology were seen near the interface; one resembled the familiar transcrystalline structure and one exhibited the shish elongated stems. Figures 6 and 7 illustrate typical higher magnification SEM images of lightly etched surfaces of the cross-sectioned sheared composite sample, showing these two morphologies at the fiber–matrix interface. The transcrystalline morphology appeared as stacked lamellae arranged perpendicularly to the fiber axis (Fig. 6) and the shish morphology appeared as a set of parallel marks aligned parallel to the fiber axis (Fig. 7). Both of these morphologies can occur side by side at different interfacial regions as shown by the model in Li et al.[18]

DISCUSSION

The *in situ* WAXD profiles of the sheared samples showed a significant level of anisotropy in the iPP domains relative to the shear direction, which is similar to our previously reported results on shear-induced crystallization in iPP containing short UHMWPE extended chain fibers.[12] The analysis of the WAXD data therein, including azimuthal profiles of

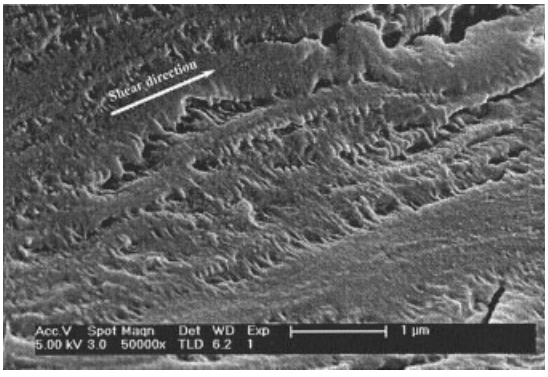

Figure 4 A high-resolution SEM image of an etched surface of a sheared iPP/AF sample, indicating the shear direction and showing the typical shish kebab morphology.

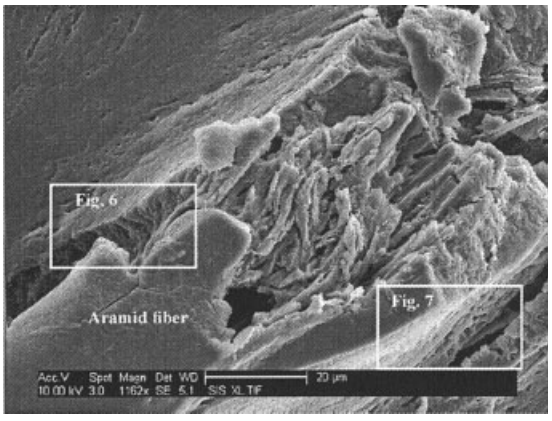

Figure 5 A high-resolution SEM image of an etched tapered cross section, showing an example of exposed fiber and the iPP matrix at the vicinity of its surface.

iPP microbeam WAXD reflections presented as a function of lateral displacement from the interface, supported the morphological observations of orientated cylindritic structures, indicative of the shish kebab morphology, which dominate the iPP matrix. Hence, the effect of shear on the matrix is similar to that observed before and even in pure iPP. From the viewpoint of orientation, the transcrystallinity of iPP on oriented AFs should give an identical WAXD pattern to the shish kebab and these patterns cannot sort between transcrystallinity and shear effects in an oriented system. Yet, such sorting is clearly feasible by the WAXD and SAXS kinetics data, as discussed later.

Based on results in Figures 1 and 2, it is apparent that the presence of short AFs facilitates the crystallization/orientation kinetics of the surrounding iPP matrix. The possible mechanism for this behavior is as follows. During shear, the principal axis of the AFs tends to align with the flow direction. Because the induction time for transcrystallization is significantly shorter than for bulk crystallization (with a time scale of many hours under quiescent conditions at 145°C), the resulting combined effect is to facilitate orientated crystallization and morphology formation. The results in Figure 1 show that, due to the fiber presence alone, a significant proportion of crystalline structure appears already after 30 min, which reduces further to about 5 min under the effect of shear. However, as seen from the results of the sheared pure iPP sample, the effect of shear alone cannot account for the extremely fast crystallization kinetic. This suggests additive effects of shear and transcrystallization.

A similar argument can be made on the basis of the SAXS results in Figure 2, regarding the development of an orientated crystalline structure. Under the effect of shear alone, a clear orientated morphology is already developed after 10 min, which reduces to 3 min in the presence of short AFs. This is comparable to our previously reported results on shear-induced crystallization in iPP containing short UHMWPE extended chain fibers.[12]

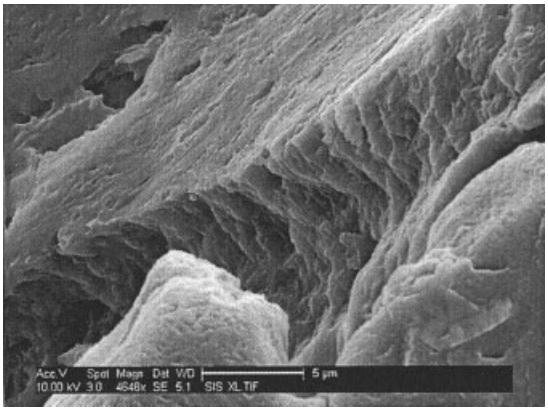

Figure 6 A higher magnification SEM image of Figure 5, showing the transcrystalline/kebab morphology that appears as stacked lamellae perpendicular to the fiber axis.

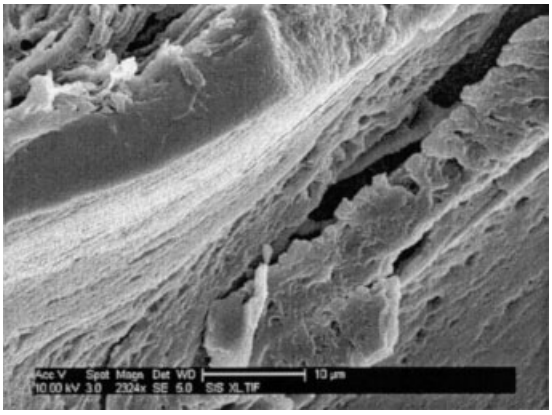

Figure 7 A higher magnification SEM image of Figure 5, showing the shish morphology that appears as a set of parallel marks along the fiber axis.

Finally, the results of the thermal analysis, which support these conclusions, are considered significant, despite the small changes in the degree of crystallinity and melting point that are attributed to shear. This is due to the fact that the thermal analysis reflects the total crystallinity, including the spherulitic crystallinity that forms upon cooling to ambient temperature following the isothermal process at 145°C and that would tend to mask the effect of the orientated crystallinity.

CONCLUSIONS

The presence of short AFs in iPP significantly enhanced shear-induced crystallization and orientation of the iPP matrix. The results indicated that the effect of shear flow on the consequential crystalline morphology comprised two separate components. The first was the typical orientation of the iPP molecules in the flow direction to form the aligned shish structure almost immediately after the application of shear. The second was the alignment of the fibers in the flow direction, parallel to the shish structure. These two components generated two corresponding nucleation and orientated crystallization processes, one with the kebab morphology on the shish entities, and another with the transcrystalline structure on the fiber surface. The resultant nucleating effect of the two components was additive, as expressed by the extremely short crystallization time of sheared AF–iPP compositions. At 145°C, the time scale for the appearance of an orientated iPP morphology was approximately 3 min.

The research of the Israeli authors was supported by the Israel Science Foundation. The U.S. team thanks the National Science Foundation for financial support. The third

author (C.A.O.) acknowledges a postdoctoral fellowship from CONACYT.

References

1. Yamazaki, S.; Watanabe, K.; Okada, K.; Yamada, K.; Tagashira, K.; Toda, A.; Hikosaka, M. Polymer 2005, 46, 1675.
2. Folkes, M. J.; Russell, D. A. M. Polymer 1980, 21, 1252.
3. Keller, A.; Kolnaar, H. W. H. Mater Sci Technol 1997, 18, 189.
4. Thomason, J. L.; Van Tooyen, A. A. J Mater Sci 1992, 27, 889.
5. Somani, R. H.; Hsiao, B. S.; Nogales, A.; Srinivas, S.; Tsou, A. H.; Sics, I.; Balta-Calleja, F. J.; Ezquerra, T. A. Macromolecules 2000, 33, 9385.
6. Somani, R. H.; Yang, L.; Hsiao, B. S.; Fruitwala, H. J. Macromol Sci Phys 2003, B42, 515.
7. Somani, R. H.; Yang, L.; Hsiao, B. S.; Agarwal, P. K.; Fruitwala, H.; Tsou, A. Macromolecules 2002, 35, 9096.
8. Somani, R. H.; Yang, L.; Hsiao, B. S. Physica 2002, A304, 145.
9. Somani, R. H.; Hsiao, B. S.; Nogales, A.; Fruitwala, H.; Srinivas, S.; Tsou, A. Macromolecules 2001, 34, 5902.
10. Nogales, A.; Hsiao, B. S.; Somani, R. H.; Srinivas, S.; Tsou, A. H.; Balta-Calleja, F. J.; Ezquerra, T. A. Polymer 2001, 42, 5247.
11. Agarwal, P. K.; Somani, R. H.; Weng, W.; Mehta, A.; Yang, L.; Ran, S.; Liu, L.; Hsiao, B. S. Macromolecules 2003, 36, 5226.
12. Dikovsky, D.; Marom, G.; Avila-Orta, C. A.; Somani, R. H.; Hsiao, B. S. Polymer, 2005, 46, 3096.
13. Assouline, E.; Fulchiron, R.; Gerard, J.-F.; Wachtel, E.; Wagner, H. D.; Marom, G. J Polym Sci Part B: Polym Phys 1999, 37, 2534.
14. Dean, D. M.; Rebenfeld, L.; Register, A.; Hsiao, B. S. J Mater Sci 1998, 33, 4797.
15. Assouline, E.; Wachtel, E.; Grigul, S.; Lustiger, A.; Wagner, H. D.; Marom, G. Macromolecules 2002, 35, 403.
16. Assouline, E.; Wachtel, E.; Grigull, S.; Lustiger, A.; Wagner, H. D.; Marom, G. Polymer 2001, 42, 6231.
17. Avila-Orta, C. A.; Somani, R.; Yang, L.; Burger, C.; Marom, G.; Hsiao, B. S. Polymer, to appear.
18. Li, Z. M.; Li, L. B.; Shen, K. Z.; Yang, W.; Huang, R.; Yang, M. B. Macromol Rapid Commun 2004, 25, 553.
19. Yang, L.; Somani, R. H.; Sics, I.; Hsiao, B. S.; Kolb, R.; Fruitwala, H.; Ong, C. Macromolecules 2004, 37, 4845.
20. Bassett, D. C.; Hodge, A. M. Proc R Soc Lond 1981, A377, 25.